URSI AP-RASC, Sydney, Australia, 17 – 22 August 2025

FOA Localization with Adaptive Frequency Offset Correction

Takeshi Amishima[(1)]
(1) Meiji University, Kanagawa, Japan; e-mail: amishima@meiji.ac.jp

Abstract

This paper addresses receiver localization using Frequency Of Arrival(FOA) from Low Earth Orbit (LEO) satellite signals, focusing on biased frequency offsets from down-conversion errors, which cause large localization errors. FOA-SFOE is needed when offsets exist, but applying it unnecessarily degrades accuracy compared to FOA localization With No Frequency Offset (FOA-WNFO). To address this, we propose a method that switches between these algorithms based on the estimated frequency offset. Numerical simulations confirm that the proposed method achieves lower localization Root Mean Squared Error (RMSE) than both FOA-WNFO and FOA localization with Simultaneous Frequency Offset Estimation (FOA-SFOE).

1. Introduction

Various localization techniques use measurements from moving platforms like Unmanned Aerial Vehicle(UAV), airplanes, Low Earth Orbit (LEO), and Geostationary Earth Orbit(GEO) satellites [1]-[14]. A common method is Time-Difference of Arrival(TDOA)/Frequency-Difference of Arrival(FDOA), which requires synchronized multiple platforms [1][2]. Alternatively, FOA-based localization uses a single moving platform, tracking an emitter over time [4]-[14]. This method is cost-effective as it avoids synchronization and multiple platforms.

Recently, the rise of LEO satellites has driven interest in localization using their downlink signals [13][14]. LEO satellites offer stronger signals than Global Navigation Satellite System (GNSS), rapid configuration changes, and high-speed motion, making Doppler frequency detection easier.

When detecting the Doppler frequency from the downlink signal, biased frequency offsets arise due to residual errors in carrier frequency removal. These offsets result from receiver oscillator errors and discrepancies between the satellite's nominal and actual transmission frequencies. Studies [7][8][9][10][16] assume no frequency offset in FOA localization, while [5][6][11][12] consider offsets and propose a method that estimates them. The former is termed FOA localization With No Frequency Offset (FOA-WNFO), and the latter FOA localization with Simultaneous Frequency Offset Estimation (FOA-SFOE).

FOA-WNFO is expected to achieve higher localization accuracy than FOA-SFOE by estimating fewer unknowns. This paper verifies the hypothesis. If the frequency offset is small, FOA-WNFO improves accuracy, though some impact remains. For large offsets, FOA-SFOE is preferable. Using both methods appropriately ensures high-precision localization.

This paper proposes a high-precision localization method that switches between FOA-WNFO and FOA-SFOE based on the estimated frequency offset. If the offset is small, FOA-WNFO is used; if large, FOA-SFOE results are selected.

2. Conventional FOA localization methods

This chapter reviews two conventional FOA-based localization methods using a single moving observation platform.

2.1. FOA localization With No Frequency Offset (FOA-WNFO)

In this section, we describe the localization method which treats the frequency offset f_{offset} as zero[7][8][9][10][16]. We will refer to it as FOA localization With No Frequency Offset (FOA-WNFO) hereafter. We start with the following observation model. Let $t_k (k=1,...,K)$ denote the observation time and define the observation model at time t_k by the following equation.

$$z(t_k) = g(t_k) + v(t_k) \tag{1}$$

$$g(t_k) = \frac{1}{\lambda} \frac{(\mathbf{v}_{sat}(t_k))^T (\mathbf{p}_t - \mathbf{p}_{sat}(t_k))}{\|(\mathbf{p}_t - \mathbf{p}_{sat}(t_k))\|} \tag{2}$$

Here, $z(t_k)$ represents the FOA, or Doppler observation, $g(t_k)$ represents the true FOA value, $v(t_k)$ represents the random observational error due to thermal noise, λ represents the wavelength, $\mathbf{p}_t$ represents the 3-dimensional position vector of the unknown radio source, and $\mathbf{p}_{sat}(t_k)$ and $\mathbf{v}_{sat}(t_k)$ represent the 3-dimensional position and velocity vectors of the moving observer platform, respectively. Additionally, we assume that $E\{v^2(t_k)\} = \sigma_{FOA}^2$ and $E\{v(t_k)\} = 0$. It is noted that the random observational error due to thermal noise refers to the frequency error caused by fluctuations in frequency due to thermal noise at the receiver[15].

Next, we impose the constraint that the radio wave source exists on the Earth's surface, using the following equation.

$$\|\mathbf{p}_t\| = R_E \tag{3}$$

Considering the constraint that the receiver exists on the Earth's surface, any position on the Earth's surface is uniquely determined by two variables: latitude and longitude. Therefore, instead of $\mathbf{p}_t$ defined in the ECEF coordinate system, we define a vector $\boldsymbol{\chi}$ of two variables in the POLAR coordinate system. Since ECEF and POLAR imply that they have the same meaning but differ only in coordinates, we will interchange them as needed hereafter. We define $\boldsymbol{\chi}_t$ as the following vector with latitude and longitude elements.

$$\boldsymbol{\chi}_t = (Lon_t \quad Lat_t)^T \tag{4}$$

To find $\boldsymbol{\chi}_t$, we solve the following weighted least squares method[17].

$$\min_{\boldsymbol{\chi}_t} J(\boldsymbol{\chi}_t, \mathbf{p}_{sat}(t_k)) \tag{5}$$

$$J(\boldsymbol{\chi}_t, \mathbf{p}_{sat}(t_k)) = \sum_{k=1}^{K} (z(t_k) - g(\boldsymbol{\chi}_t, \mathbf{p}_{sat}(t_k)))\sigma_{FOA}^{-2}(z(t_k) - g(\boldsymbol{\chi}_t, \mathbf{p}_{sat}(t_k))) \tag{6}$$

2.2. FOA localization with Simultaneous Frequency Offset Estimation (FOA-SFOE)

In the localization method presented in this section, the frequency offset is treated as an unknown variable[5][6][11][12]. Henceforth, it will be referred to as FOA localization with Simultaneous Frequency Offset Estimation (FOA-SFOE). Instead of (2), we consider the following observation model with frequency offset f_{offset}.

$$h(t_k) = f_{offset} + \frac{1}{\lambda}\frac{(\mathbf{v}_{sat}(t_k))^T(\mathbf{p}_t - \mathbf{p}_{sat}(t_k))}{\|(\mathbf{p}_t - \mathbf{p}_{sat}(t_k))\|} \tag{7}$$

Hereafter $g(t_k)$ term in (1) also is replaced by $h(t_k)$. Let us define the following unknown variable vector along with $\boldsymbol{\chi}_t$.

$$\bar{\boldsymbol{\chi}}_t = \begin{pmatrix} \boldsymbol{\chi}_t \\ f_{offset} \end{pmatrix} \tag{8}$$

To determine $\bar{\boldsymbol{\chi}}_t$, we solve the following weighted least squares minimization [17].

$$\min_{\bar{\boldsymbol{\chi}}_t} J(\bar{\boldsymbol{\chi}}_t, \mathbf{p}_{sat}(t_k)) \tag{9}$$

$$J(\bar{\boldsymbol{\chi}}_t, \mathbf{p}_{sat}(t_k)) = \sum_{k=1}^{K} (z(t_k) - h(\bar{\boldsymbol{\chi}}_t, \mathbf{p}_{sat}(t_k)))\sigma_{FOA}^{-2}(z(t_k) - h(\bar{\boldsymbol{\chi}}_t, \mathbf{p}_{sat}(t_k))) \tag{10}$$

3. The proposed Switching FOA localization based on the Estimated Frequency Offset (SFOA-EFO)

When the frequency offset is small, FOA-WNFO may yield lower localization errors than FOA-SFOE. However, when the offset is significant, FOA-SFOE is more appropriate as FOA-WNFO's accuracy deteriorates. To address this, we propose Switching FOA Localization based on Estimated Frequency Offset (SFOA-EFO).

Fig. 1 outlines the process: FOA-WNFO is used if the offset is small, while FOA-SFOE is selected if the offset is large. The switching conditions are as follows:

$$\hat{f}_{offset} < N\hat{\sigma}_{foffset} \tag{11}$$

Here, $\hat{\sigma}_{foffset}$ is a value calculated from the theoretical expression for the estimation error of the frequency offset. Furthermore, N is a threshold-setting parameter, and $\hat{f}_{offset}$ represents the estimated frequency offset value, which is estimated by FOA-SFOE method described in Section 2.2. Note that in (11), the variables are expressed with $\hat{}$ since they are based on the estimated values, namely, localization results and satellite position and velocity information are also estimated from the orbital determination.

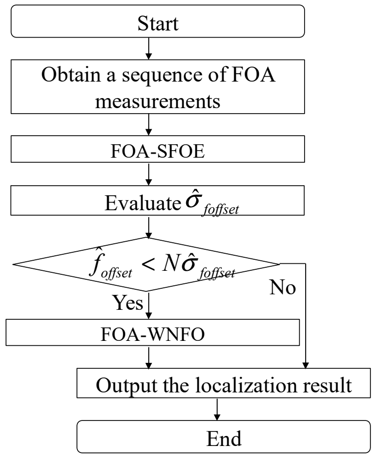

Fig. 1 The processing flow of the proposed method.

4. Computational simulation

This chapter presents computational simulations to evaluate the proposed method and compare it with conventional approaches.

4.1. Simulation conditions

This section outlines the default simulation conditions. Table 1 lists the parameter values, and Fig. 2 illustrates the LEO satellite-receiver geometry.

Localization occurs as the FOA satellite passes over New South Wales, with the receiver in Sydney. LEO satellite position and velocity errors follow normal distributions with standard deviations of 10m and 0.1m/s per axis. FOA measurements span 20 seconds at 0.2-second intervals, yielding 101 measurements. Measurement errors follow a normal distribution with a 1.0 Hz standard deviation. The threshold parameter is set to 2.0, and 1000 Monte Carlo iterations are performed.

Table 1 Default simulation parameter values.

Parameters	Values
LEO satellite orbit parameters	Altitude approximately 868.1 km, passing over New South Wales from northwest to southeast at a speed of approximately 7.12 km/s. (Calculated from NORAD 2-line elements [20])
Position Error (σ)	(10m,10m,10m)
Velocity Error (σ)	(0.1m/s,0.1m/s,0.1m/s)
Receiver location	
Latitude, Longitude	Sydney (33.595°S, 151.17°E)
FOA measurement parameters	

Measurement duration	20.0sec
Measurement interval	0.2sec
Measurement error (σ)	1.0Hz
Frequency offset	0Hz and 500 Hz (2cases)
SFOA-EFO Parameters	
Threshold Setting Parameter $_N$	2.0
Other	
Number of Monte Carlo Iterations	1000times

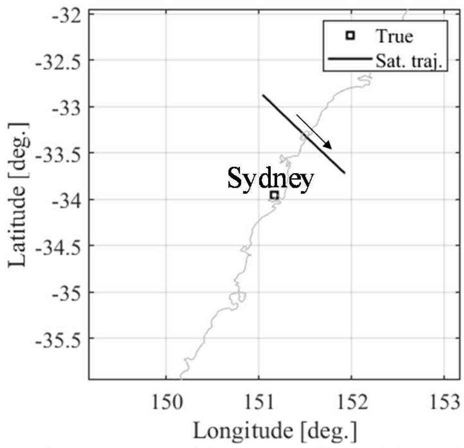

Fig. 2 Geometry of the LEO satellite and the receiver.

4.2. Example of simulation results under default conditions

This section presents simulation results under default conditions. Table 2 shows the RMSE for FOA-WNFO, FOA-SFOE, and the proposed SFOA-EFO, while Table 3shows the selection proportions of FOA-WNFO and FOA-SFOE in SFOA-EFO. Fig. 3 to Fig. 5 illustrate the localization results from Monte Carlo iterations, zoomed near the receiver.

For FOA-WNFO and FOA-SFOE, when the frequency offset is 0 Hz, FOA-WNFO gives a smaller RMSE of 0.56km, but at 500 Hz, the RMSE increases to 4.56 km due to the 0 Hz assumption. Fig. 3(b) shows a consistent directional error in FOA-WNFO at 500 Hz.

FOA-SFOE, as shown in Fig. 4, provides similar RMSE (1.55 km at 0 Hz and 1.57 km at 500 Hz).

For SFOA-EFO, when the frequency offset is 0 Hz, the RMSE is 0.72km (comparable to FOA-WNFO), and at 500 Hz, the RMSE is 2.28 km (comparable to FOA-SFOE). This switching approach ensures good localization accuracy by selecting the appropriate method based on the frequency offset.

Furthermore, we evaluate the RMSE reduction rate quantitatively. Using the result shown in Table 2, when f_{offset} =0Hz, the RMSE reduction rate is:

$$\frac{(FOA-SFOE)-(SFOA-EFO)}{FOA-SFOE}\times 100 = 53.55\% \quad (12)$$

In the same manner, when f_{offset} =500Hz, the RMSE reduction rate is:

$$\frac{(FOA-WNFO)-(SFOA-EFO)}{FOA-WNFO}\times 100\% = 54.34\% \quad (13)$$

RMSE was reduced from 1.55 km to 0.72 km at 0 Hz (53.55% improvement) and from 4.56 km to 2.28 km at 500 Hz (54.34% improvement). Additionally, Table 3 shows that FOA-WNFO was chosen 97.70% of the time at 0 Hz, while FOA-SFOE was selected 82.20% of the time at 500 Hz. These results demonstrate that switching methods based on frequency offset reduces localization errors.

Table 2 RMSE for FOA-WNFO, FOA-SFOE, and proposed FOA-SFOE method (Theoretical values).

Method \ f_{offset}	0Hz	500Hz
FOA-WNFO	0.56km (0.55km)	4.56km
FOA-SFOE	1.55km (1.57km)	1.57km (1.57km)
SFOA-EFO	0.72km	2.28km

Table 3 Proportion of selection of FOA-WNFO and FOA-SFOE under the proposed FOA-SFOE Method.

Method \ f_{offset}	0Hz	500Hz
FOA-WNFO	97.70%	2.30%
FOA-SFOE	17.80%	82.20%

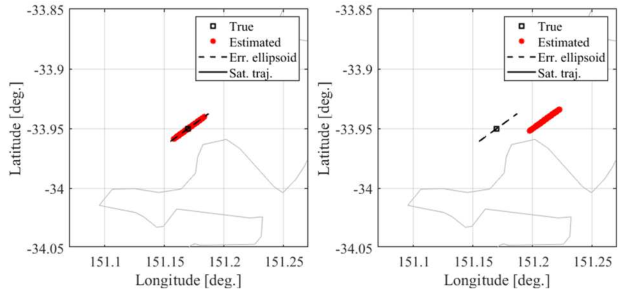

(a) f_{offset} =0Hz (b) f_{offset} =500Hz

Fig. 3 Localization results from Monte Carlo iterations of FOA-WNFO.

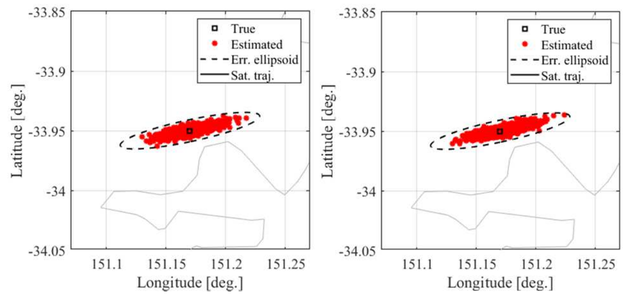

(a) f_{offset} =0Hz (b) f_{offset} =500Hz

Fig. 4 Localization results from Monte Carlo iterations of FOA-SFOE.

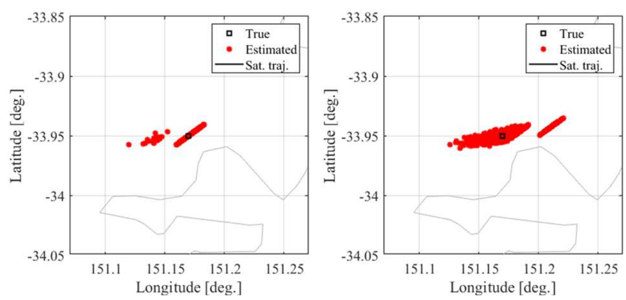

(a) f_{offset} =0Hz (b) f_{offset} =500Hz

Fig. 5 Localization results from Monte Carlo iterations of the proposed SFOA-EFO.

5. Conclusions and remarks

In this paper, we proposed a FOA-based localization method that reduces the effect of biased frequency offset by switching between two localization methods based on the estimated offset. Numerical simulations confirmed its effectiveness, with FOA-WNFO selected for low offsets and FOA-SFOE for high offsets.

A remaining challenge is optimizing the threshold parameter, which depends on frequency offset estimation accuracy. Improving estimation precision will enable more effective switching, and further research will focus on refining parameter-setting methods.

References

[1] P. Haworth, et. al., “Interference localization for Eutelsat satellites -the first European transmitter location system,” Int. J. of Sat. Comm., vol.15, pp.155–183, 1997.

[2] U. Engel, “A geolocation method using ToA and FoA measurements,” 6th Workshop on Localization, Navigation and Communication, 2009.

[3] J. Li, S. Lv, L. Yang, S. Wu, Y. Liu and Q. Luan, “Performance Analysis for Bearings-only Geolocation Based on Constellation of Satellites," 2022 IEEE International Conference on Trust, Security and Privacy in Computing and Communications (TrustCom), pp. 1429-1434, 2022.

[4] P. Ellis and F. Dowla, “A Single Satellite Geolocation Solution of an RF Emitter Using a Constrained Unscented Kalman Filter,” IEEE Statistical Signal Processing Workshop (SSP), 2018.

[5] A. Yamanaka and H. Ishikawa, “Performance Evaluation of Frequency Offset Compensation Method for Doppler Shift Multiple Observations in User Position Detection System using Unmanned Aerial Vehicles,” IEICE Technical Report, vol. 121, no. 379, SAT2021-59, pp. 39-44, 2022.

[6] A. Yamanaka and H. Ishikawa, “Performance evaluations of frequency offset compensation technique for user position detection system using unmanned aerial vehicles,” IEICE Technical Report, vol. 121, no. 152, SAT2021-32, pp. 21-26, August 2021.

[7] H. Ishikawa, Y. Horikawa, and H. Shinonaga, “Performance Evaluation of Maximum Estimation Error of User Position Detection Method using Single Unmanned Aerial Vehicle,” IEICE Technical Report, vol. 119, no. 220, SAT2019-64, pp. 121-126, October 2019.

[8] S. Iwase, Y. Horiwaka, and H. Ishikawa, “Characteristic Evaluation of Position Detection Method Using One Unmanned Aerial Vehicle Based on Maximum Error Estimation Method,” IEICE Technical Report, vol. 119, no. 175, SAT2019-34, pp. 93-98, August 2019.

[9] Y. Saito and H. Ishikawa, “Performance evaluation of initial values selection algorithm for position detection method using unmanned aerial vehicles,” IEICE Technical Report, vol. 118, no. 176, SAT2018-43, pp. 79-83, August 2018.

[10] H. Ishikawa, “Study on User Position Detection Method Using One Unmanned Aerial Vehicle,” IEICE Technical Report, vol. 115, no. 180, SAT2015-25, pp. 83-88, August 2015.

[11] T. Amishima, “Theoretical FOA based geolocation accuracy by single moving platform considering orbital error,” IEICE Transactions on Communications B, Vol.J106-B, No.2, pp.88-100, 2023.

[12] T. Amishima," Localization of a moving target using the sequence of FOA measurements by a moving observation platform," IEICE TRANSACTIONS on Communications, Vol. E106.B, No. 11 pp. 1256-1265,2023.

[13] M. Neinavaie, J. Khalife and Z. M. Kassas, "Acquisition, Doppler Tracking, and Positioning With Starlink LEO Satellites: First Results," in IEEE Transactions on Aerospace and Electronic Systems, vol. 58, no. 3, pp. 2606-2610, June 2022.

[14] M. Neinavaie and Z. M. Kassas, "Unveiling Starlink LEO Satellite OFDM-Like Signal Structure Enabling Precise Positioning," in IEEE Transactions on Aerospace and Electronic Systems, vol. 60, no. 2, pp. 2486-2489, April 2024.

[15] S. M. Kay, “Fundamentals of Statistical Processing, Volume I: Estimation Theory,” Prentice Hall, 1993.

[16] Z. Qi, Z. Liyuan, H. Xu, and Guohao Zhang., “NLOS Effect on LEO Doppler Localization: A case Study in Hong Kong,” 2023 IEEE International Symposium On Antennas And Propagation, pp. 1-2, 2023.

[17] A. Gelb, "Applied Optimal Estimation,” The MIT Press,1974.

[18] K. Zhou, John C. Doyle, and K. Glover, "Robust and Optimal Control,” Prentice Hall,1995.

[19] G. Strang, “Linear Algebra and its Applications," Harcourt Brace & Company, 1986.

[20] T. S. Kelso, F. R. Hoots, and, R. L. Roehrich: Models for Propagation of NORAD Element Sets, Project Space Track Report No. 3, Dep. of Commerce National Technical Information Service, 1980.